ANALYSIS AND IMPLEMENTATION OF LARGE EDDY SIMULATION IN CFD BASED SIMULATION OF CONFINED HIGH SWIRLING FLAMES

Marko Klančišar[1]*, Tim Schloen[2], Matjaž Hriberšek[3], Niko Samec[4]

[1]Dr. Marko Klančišar, Max Weishaupt GmbH, Germany
[2]Dr. Tim Schloen, Max Weishaupt GmbH, Germany
[3]Prof. Dr. Matjaž Hriberšek, University of Maribor, Faculty of mechanical engineering, Slovenia
[4]Prof. Dr. Niko Samec, University of Maribor, Faculty of mechanical engineering, Slovenia

Abstract

This article examines the implementation of CFD technology in the design of the industrial burner with swirl flame technology and practical application of different approaches to the modeling of turbulence and combustion. The choice of the LES turbulence model over standard RANS offers a possibility to improve the quality of the combustion-flow field interaction. For the case of combustion modelling, the Eddy Dissipation Model (EDM) was selected, which can be extended to simulate combustion within LES. Depending on system requirements, especially with continuous physical processes as well as the well-known results of experimental measurements, it was possible to determine the mixing field and its intensity in the turbulent flow, the description of heat release and interaction of turbulent flow field and chemical kinetics.

1. Introduction

To overcome computing limitations in case of combustion for both temporal and spatial scales one can explore model adaptation, mesh adaptation or both at the same time. Model adaptation refers to a series of models in which the governing equations are modified to a reduced order, reduced scales or the statistical design that effectively separates and removes smaller scales from direct computation. Adaptation of the mesh refers to mesh hierarchy or mesh resolution, obtained by adjusting the mesh density according to selected error criteria. For flow-reactive coupling schemes, these model adaptations lead to three basic strategies in use: DNS, RANS and LES [1] to [3]. In order to capture most important temporal and spatial variations of combustion fields in this work the LES was selected. It is based on spatial filtering of the governing equations to capture the majority of flow structures, resulting in the transport equations for the spatially filtered mass, momentum, and scalar while the effects of the smaller scales are directly modeled, [4] to [7]. LES relies on the separation of flow structures or carriers of the turbulent kinetic energy from smaller (sub-grid) structures, which eventually dissipate into internal energy. This approach has its roots in the traditional view of turbulent flows where the majority of the turbulent kinetic energy has its source in larger scales. LES includes extensive information on both the momentum and the scalar fields and can capture larger mixing structures in the flows, e.g. in combustion [8], [9]. In the case of combustion, this approach is not without problems, as the important effects of reactive flows occur at smaller scales, where interaction with the chemical kinetics is important.

2. Computational model

2.1 *Model set-up*

The burner CAD model is introduced on the basis of the CAD model of the structural combustion system (Figure 1), and is adapted to the practical position of the dissipating mixing plate and to other elements in accordance with the experimental situations (e.g. fuel inlet position).

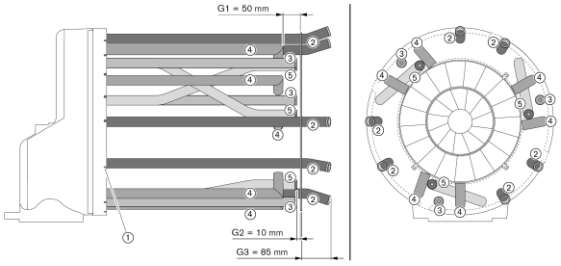

Figure 1: Fuel distribution (1-gas manifold, 2-gas nozzle ϕ 20mm, 3-gas nozzle ϕ 8mm, 4-gas nozzle ϕ 8mm, 5-gas nozzle ϕ 8mm)

Through detailed measurements, it was possible to determine the natural operational state of the burner according to the type of fuel (natural gas NG in our case). Axial and radial components were calculated from known physical characteristics of both the fuel input (tangential velocity of the fuel is assumed as 0), and the air. Turbulence is expressed by the intensity and the hydraulic diameter, which are 5% and 18 mm for the fuel inlet, and 7% and 600 mm for the air inlet. The thermal boundary conditions are transferred from the experimental hot water system (Table 1).

*Corresponding author: fg.klancisar@weishaupt.de

Average fuel mass flow	0.6122 kg/s
Average air mass flow	8.25234 kg/s
Swirl number	0.5, 0.6, 0.75
Inlet air temperature	306.0 K
Absolute pressure	95500 Pa
Fuel-Air ratio (λ)	1.15
Static pressure - outlet	20 Pa
Average temperature – combustion chamber wall	343 K

Table 1: Experimental operational conditions – natural gas

Based on conclusions from experimental measurements and development goals, that need to be achieved, the following requirements for the numerical simulations were posed:

1. Reliable calculation of the three-dimensional turbulent flow field.
2. Determination of the mixing field or its intensity in turbulent flow.
3. Description of heat release and interaction of turbulent flow field and chemical kinetics.

2.2 Computational mesh

Numerical simulation of swirled combustion was carried out on an axially symmetric domain. To compare the quality of the results we used four non-uniform computational meshes. On meshes 2, 3 and 4 (Table 2) we used a detailed discretization of near entry points and stator blades to achieve high numerical resolution. We also used symmetrical treatment of recurrent domains to achieve the appropriate quality of temporal calculations.

	Comp. mesh 1	Comp. mesh 2	Comp. mesh 3	Comp. mesh 4
Nodes	70536	228315	2251218	7523986
Elements	296251	979471	12410198	23324356

Table 2: Mesh characteristics

2.3 Reactive flow computation

Chemical and flow conditions of the system, which includes reactive flow in the gaseous phase, are described by time-dependent conservation equations of mass, species, momentum and energy. Change in density ρ is associated with the temperature and composition of the fluid; estimated by using equations of state. The turbulence was modeled by two approaches, first by the standard k-epsilon RANS model and second by using the Large Eddy Simulation (LES). In our case, in the context of LES the Wall Adapting Local Eddy-Viscosity (WALE) sub-grid model (equations (1) to (3)) was applied, as it is recommended for the use in complex geometries [10]. Based on Smagorinsky-Lilly model, WALE is useful on a wide range of flows. The Eddy viscosity in WALE is modeled as:

$$\mu_t = \rho L_s^2 \frac{\left(s_{ij}^d s_{ij}^d\right)^{\frac{3}{2}}}{\left(\bar{s}_{ij}\bar{s}_{ij}\right)^{\frac{5}{2}} + \left(s_{ij}^d s_{ij}^d\right)^{\frac{5}{4}}} \quad (1)$$

where L_s and S_{ij}^d are defined as:

$$L_s = min\left(kd, C_w V^{\frac{1}{3}}\right) \quad (2)$$

$$S_{ij}^d = \frac{1}{2}\left(\bar{g}_{ij}^2 + \bar{g}_{ji}^2\right) - \frac{1}{3}\delta_{ij}\bar{g}_{kk}^2 \quad (3)$$

Given the fact that we are dealing with non-premixed turbulent flames, the analysis requires an appropriate strategy to link the turbulent mixing with the reactions of the main species [11] to [14]. For the above mentioned, we used the Eddy Dissipation Model (EDM) [15] and [16]. Based on the oxygen balance, oxidation of NG/O_2 mixture can be shown with use of local air ratio and local levels of burnout basis. Detailed review of species CH_4, O_2, N_2, CO, H_2, CO_2 and H_2O can define different oxygen concentrations.

3. Analysis of results

3.1 Realized simulations

We studied the non-isothermal flow field and mixing field with all previously described parameters. In order to investigate the influence of swirled motion on the flow and mixing field, we performed unsteady calculations (unsteady RANS) as well as stationary calculation (RANS). According to computational mesh and the reproducibility of the physical events we selected physical iteration step Δt = 0.0001 s. Consequently (unsteady RANS), according to the variation of numerical parameters (time step, the convergence criterion), we detected strong convergence deviation soon after 1.4 cycle was complete. As mentioned before, we compensated using the implemented LES strategy with a sub-grid WALE model.

3.2 RANS – LES comparison

For studying the stability (or instability) of non-premixed combustion in the opposed swirl movement, accurate characterization of the distribution of the fuel is needed. The simulation results are showing deep penetration of near-stoichiometric species and the mixing profile of fuel and air. For display of the distribution of mixing fraction, we can distinguish between fields of primary and secondary air and fuel field (intensity of reactions). As a result of suitably modified simulations (RANS) we can observe heavy differences in the result comparison of experiment and numerical model due to mesh deformation.

RANS is not suitable for the study of local factors in so called microstructure of the flame, even if it is completely satisfactory on the global level. When using a standard k-ε model, time averaging flow field is also not comparable with experimental results. From this it can be concluded that the calculated turbulent kinetic energy is lower than the value obtained experimentally. Result basis were essentially transverse layer or rather cross-section of the combustion chamber on a distance of 1000 mm from the beginning of the combustion chamber (burner flange) calculated with the use of computational mesh 2. Consequently we observed deviations in burnout of reactants and intermediate products (CO) as in the temperature field. According to the comparison, we decided for further use of the computational mesh 3. Mesh 4 is a characteristically complex (longer computational time), but does not provide considerable improvement according to mesh 3. Due to oscillations, LES results are shown as mean temperature and CO emissions with the comparison to RANS. In addition, it is necessary to set the time step (ΔT). To ensure the accuracy, Courant number should generally be less than 1. For the time step we initially chose $\Delta T = 10^{-2}$, which has proved to be inadequate.

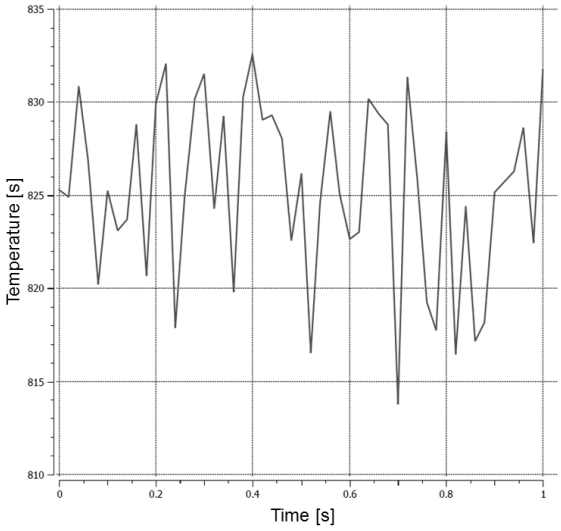

Figure 2: Temperature oscillation, 500 mm from burner flange (LES) – average temperature T_{trnavg}=832 K

Similar behavior was observed when we increased the time step on simple mesh 1, which later proved to be adequate on a redefined mesh 3. Mesh therefore has a strong influence on the accuracy and stability of LES simulation. Figures 2 - 6 are showing us temperature fluctuations of LES simulations for every 200 time steps (T_{init} = 0 s). Simulation initialization was taken from the results of the RANS simulation (computational mesh 3), which has proved to be satisfactory, as all the LES initial conditions (e.g. RMS velocity fluctuations) could not be estimated with sufficient accuracy [17] to [19]. Boundary conditions of inlet, outlet and wall were already shown in Table 1. Figure 2 shows the temperature fluctuations at central burner point with a distance of 500 mm from the burner flange. At this point we used mesh 3, which differs from the RANS mesh in the quality and number of cells (the same applies for other LES computational meshes).

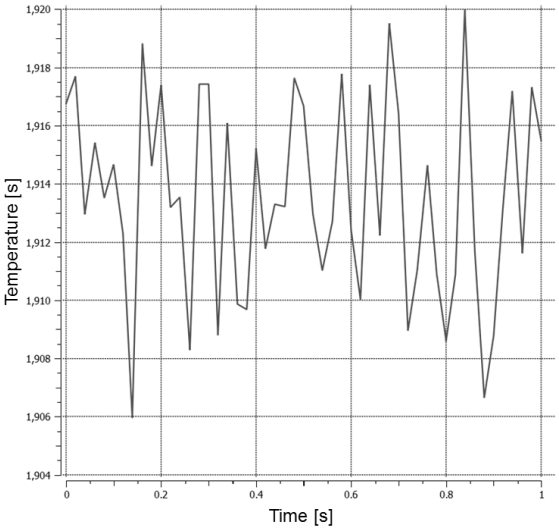

Figure 3: Temperature oscillation, 1500 mm from burner flange (LES) – average temperature T_{trnavg}=1915 K

We can observe that the maximum deviation from the average value (the "T_{trnavg}" or time-dependent Arithmetic mean) is up to 19 K. This can be attributed to the intense mixing and very fast chemical kinetics. This marks also the beginning of the flame core, which is the most stable in its center (Figure 3). Temperature deviations from the average value, are relatively small (on average, about 5 K), which already shows a stable flame with small oscillations. Another example can be seen in Figure 4 where oscillations are similar to that in Figure 3, though at a distance of three meters from the burner flange. In Figure 5 the reference point has its distance of 6000 mm from the burner flange. Oscillations increases as we're slowly coming to a burnout zone where in addition to "weakening" of chemical kinetics we can observe strong decrease of the swirl strength. This directly results in weaker flame stability and greater temperature fluctuations.

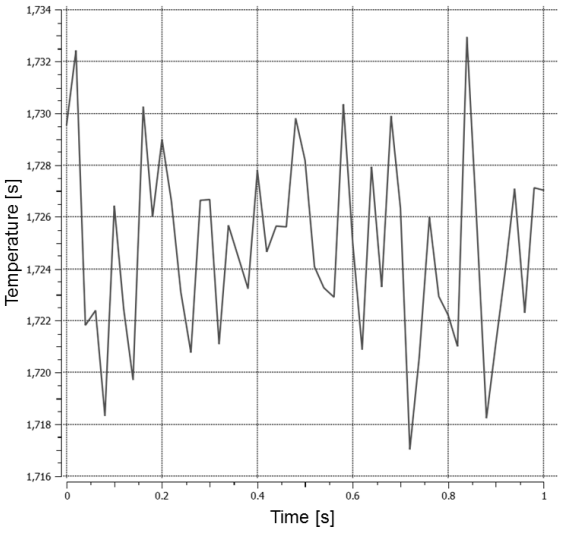

Figure 4: Temperature oscillation, 3000 mm from burner flange (LES) – average temperature T_{trnavg}=1725 K

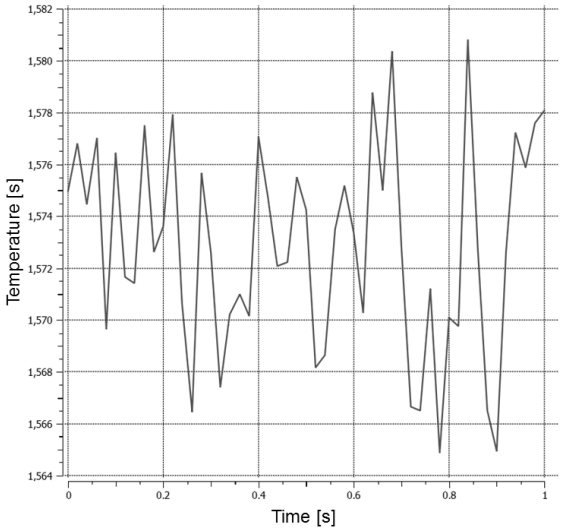

Figure 5: Temperature oscillation, 6000 mm from burner flange (LES) – average temperature T_{trnavg}=1573 K

With help of Figures 2-5 we can determine that the weakest deviation from the average value occurs halfway through the simulation time. This "harmonic oscillation" shown in these four figures can be extrapolated or one can expect a recurrence with use of longer simulation time. This phenomenon can be attributed to a slight pulsation of the flame.

Figure 6 shows the reactive zone, where the chemical kinetics is very weak. Deviations have been there before as shown on previous figures, but we can note similar behavior as in the initial field in Figure 2.

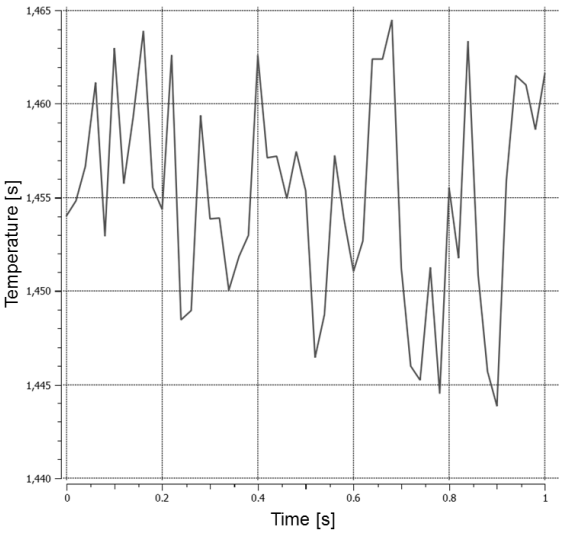

Figure 6: Temperature oscillation, 7500 mm from burner flange (LES) – average temperature T_{trnavg}=1456 K

3.3 Analogy with experimental results

In our case, the temporal flow is repeatable or periodic which means that unsteady RANS must be averaged within one time period for comparison with the averaged data. In comparison with the LES the time scales are completely different. CFD simulations reproduced with the LES method and WALE sub-grid model are showing much better comparison or numerical similarity with the experiment, which can be confirmed by comparing the RANS and LES temperature fields with the experimental data (Figures 7-10).

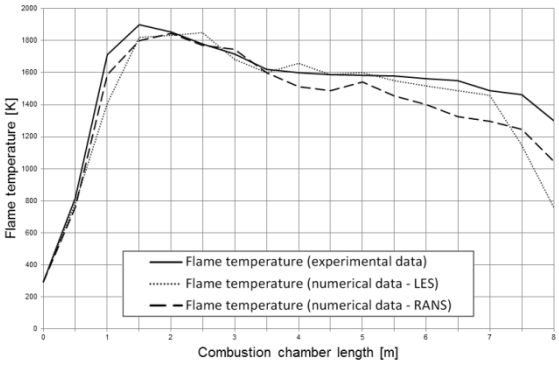

Figure 7: Comparison between experimental, RANS and LES results (temperature) – computational mesh 1

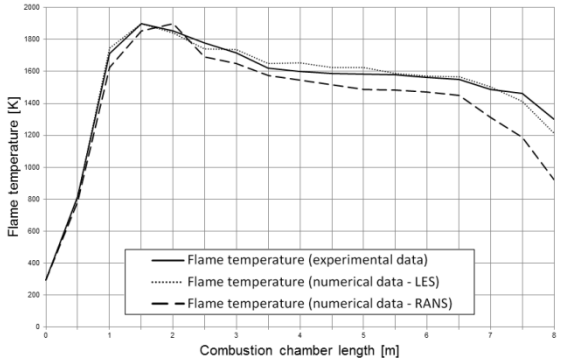

Figure 8: Comparison between experimental, RANS and LES results (temperature) – computational mesh 2

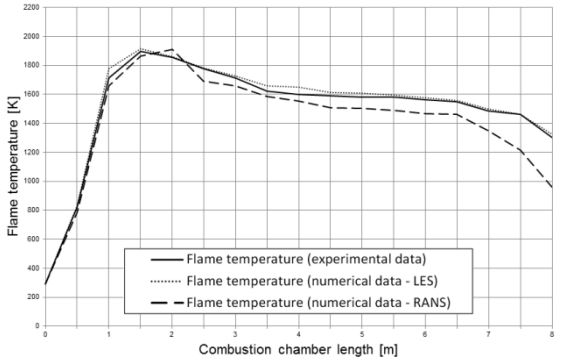

Figure 9: Comparison between experimental, RANS and LES results (temperature) – computational mesh 3

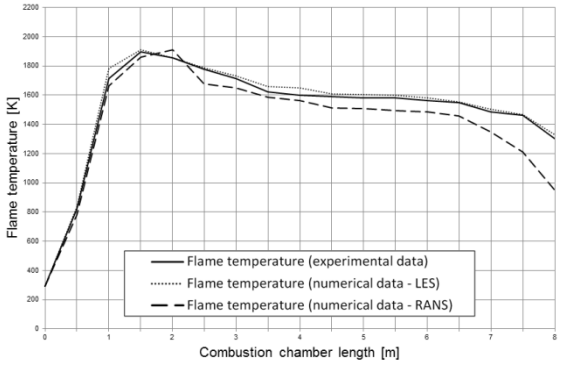

Figure 10: Comparison between experimental, RANS and LES results (temperature) – computational mesh 4

We can verify the quality of a selected mesh by comparison of the RANS and LES data with use of different computational mesh. Figure 11 is showing us a comparison of temperature trends in the longitudinal axis of the combustion chamber, where it can be seen that the mesh 1 is showing a strong deviating behavior apart from the other three. However, since the other three meshes do not show significant deviations (in our case according to level of accuracy), the mesh 2 partially and mesh 3 completely satisfies our accuracy needs.

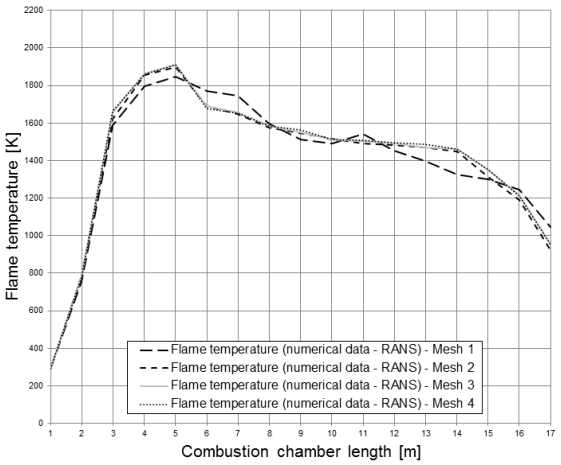

Figure 11: Comparison of temperature trends between meshes 1, 2, 3 and 4 - RANS

Similar behavior can be observed on LES example in Figure 12, where the mesh 1 again shows a significant deviation from the other meshes. As we mentioned, for LES simulations compared with RANS quality and fineness of mesh is even more important, as can be seen from the presented relations. Computational mesh is in our case completely satisfactory, but in the burnout zone (at the end of the combustion chamber) we can still observe slight deviations from the uniform trend of meshes 3 and 4.

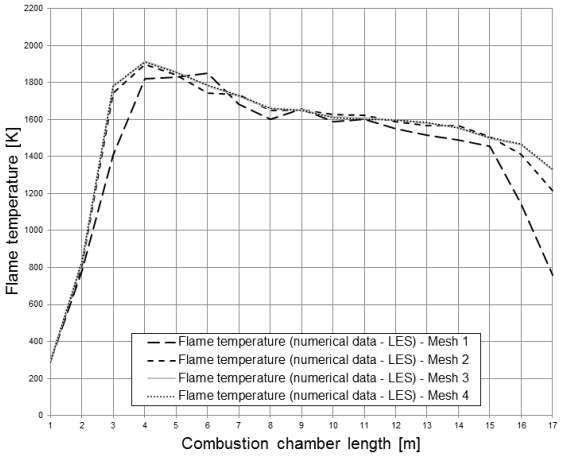

Figure 12: Comparison of temperature trends between meshes 1, 2, 3 and 4 – LES

4. Conclusion and discussion

Even when we used a denser discretization of the computational mesh (in RANS case), the low quality of mesh 1 resulted in large oscillations of the recorded average values. Where we (the LES case), with the use of mesh 3, detected deviations up to 20K (slightly over 2%), we observed with use of mesh 3 and the RANS method, deviations of up to 100K (over 12%). Of course, variations may be attributed to pulsations and fluctuations in the flame itself, but the examples on Figures 2-6 are showing the fact that

the local temperature fluctuations are relatively small. In our case, the flow is time periodic which means that unsteady RANS must be averaged within one time period for comparison with the averaged data. In comparison with the LES, the time schemes are completely different. LES resolves vortices in turbulence itself, while the unsteady RANS resolves only the structure of the flow. Consequently, LES requires a much denser spatial (mesh) and temporal resolution. Finally we conclude that RANS is sufficient for prediction of global parameters, but for the study of critical areas of intense mixing, strong turbulence and rapid chemical kinetics, it is not accurate enough and should be replaced by LES.

5. References

[1] Škerget, L., Hribersek, M. (1999). Computational fluid dynamics by Boundary-domain integral method. *International Journal for Numerical Methods in Engineering*, 46, 1291-1311, DOI: 10.1002/(SICI)1097-0207(19991120)

[2] Gerlinger, P. (2005). Numerische Verbrennungs simulation, Springer, Berlin Heidelberg

[3] Poinsot, T., Veynante, D. (2005). Theoretical and Numerical combustion, Edwards, Philadelphia.

[4] Giauque, A., Selle, L., Poinsot, T., Buechner, H., Kaufmann, P., Krebs, W., (2005). System identification of a large-scale swirled partially premixed combustor using LES and measurements, *Journal of Turbulence*, p. 1-20, DOI: 10.1080/14685240512331391985.

[5] Poinsot, T., (2010). Numerical and Physical Instabilities in Massively Parallel LES of Reacting Flows, *Journal of Scientific Computing*, Vol 49., p. 78-93, DOI: 10.1007/s10915-010-9432-8.

[6] Colin, O., Ducros, F., Veynante, D., Poinsot, T., (2000). A thickened flame model for Large Eddy Simulations of turbulent premixed combustion. *Physics of Fluids*. Vol. 12(7), p. 1843–1863, DOI:10.1063/1.870436.

[7] Roux, S., Lartigue, G., Poinsot, T., Meier, U., Bérat, C., (2005). Studies of mean and unsteady flow in a swirled combustor using experiments, acoustic analysis and Large Eddy Simulations. *Combustion and Flame*. Vol. 141, p. 40–54, DOI:10.1016/j.combustflame.2004.12.007.

[8] Vervisch, L. (2005), Turbulent Combustion Modeling, *2005 INRIA Conference Proceedings*, p. 2-43.

[9] Zhang, F., Habisreuther, P., Hettel, M., Bockhorn, H., (2009). Modelling of a premixed swirl-stabilized flame using a turbulent flame speed closure model in LES, *Flow Turbulence Combustion*, Vol. 82, p. 537–55, DOI:10.1007/s10494-008-9175-x.

[10] Klančišar, M., Goebel, D., Schloen, T., Hriberšek, M., Samec, N., (2013). Prediction of mean scalar values and CO-/NOX emissions from confined non-premixed swirl flames with CFD based simulation. *BWK Brennstoff-Wärme-Kraft*, Vol. 10, p. 38-43.

[11] Wetzel, F., (2007). Numerical investigations for stabilisation of non-premixed, dual swirled flames, Doctoral dissertation, University of Karlsruhe, Karlsruhe.

[12] Huang, Y., Sung, H.G., Hsieh, S.Y., Yang, V., (2003). Large Eddy Simulation of combustion dynamics of lean-premixed swirl-stabilized combustor. *Journal of Propulsion and Power*, Vol. 19(5), p. 782–794, DOI:10.2514/2.6194.

[13] Baum, M., Poinsot, T. J., Thevenin, D., (1994). Accurate boundary conditions for multispecies reacting flows. *Journal of Computational Physics* Vol. 116, p. 247-261.

[14] Sommerer, Y., Galley, D., Poinsot, T., Ducruix, S., Lacas, F., Veynante, D., (2004). Large eddy simulation and experimental study of flashback and blow-off in a lean partially premixed swirled burner. *Journal of Turbulence*, Vol. 5, DOI: 10.1088/1468-5248/5/1/037.

[15] Staffelbach, G., Poinsot, T., (2006). High performance computing for combustion applications. *Super Computing 2006*. Tampa, Florida, USA, DOI:10.1145/1188455.1188514.

[16] Caraeni, D., Bergstrom, C., Fuchs, L., (2000). Modeling of liquid fuel injection, evaporation and mixing in a gas turbine burner using large eddy simulation. *Flow, Turbulence And Combustion*. Vol. 65, p. 223-244, DOI:10.1023/A:1011428926494.

[17] Senoner, J.M., García, M., Mendez, S., Staffelbach, G., Vermorel, O., Poinsot, T., (2008). Growth of rounding errors and repetitivity of Large-Eddy Simulations. *AIAA Journal*, Vol. 46(7), p. 1773–1781, DOI:10.2514/1.34862.

[18] Vreman, B., Geurts, B., Kuerten, H., (1996). Comparison of numerical schemes in large-eddy simulation of the temporal mixing layer. *International Journal for Numerical Methods in Fluids*, Vol. 22, p. 297–311, DOI:10.1002/(SICI)1097-0363(19960229)

[19] Sagaut, P., (2000). Large Eddy Simulation for incompressible flows. Scientific computation series. Springer-Verlag.